

# **Nickel Hydroxide/Sulfide Hybrids: Halide Ion Controlled Synthesis, Structural Characteristics, and Electrochemical Performance**

Qibin Wu,<sup>a,c</sup> Weining Li,<sup>a</sup> Xuefeng Zou,<sup>\*b</sup> Bin Xiang<sup>\*a</sup>

<sup>a</sup>Chemistry and Chemical Engineering, Chongqing University, Chongqing 400044, China.

<sup>b</sup>Guizhou Provincial Key Laboratory of Computational Nano-Material Science, Guizhou Education University, Guiyang 550018, China.

<sup>c</sup>State Key Laboratory of Advanced Chemical Power Sources, Guizhou Meiling Power Sources Co. Ltd., Zunyi, Guizhou 563003, China.

\*Corresponding Author.

E-mail: njzouxf@gznc.edu.cn (X. Zou), xiangbin@cqu.edu.cn (B. Xiang)

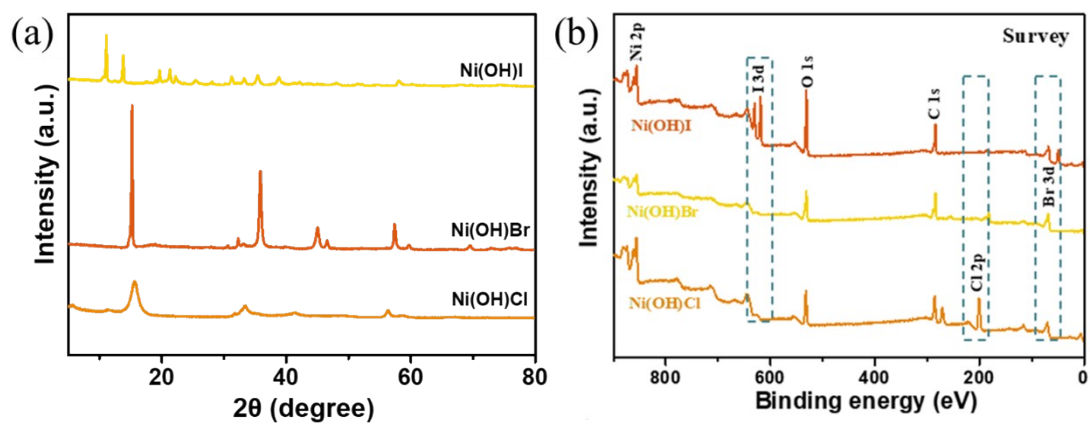


**Figure S1.** (a) XRD patterns of Ni(OH)Cl, Ni(OH)Br and Ni(OH)I. (b) XPS spectra of Ni(OH)Cl, Ni(OH)Br and Ni(OH)I.

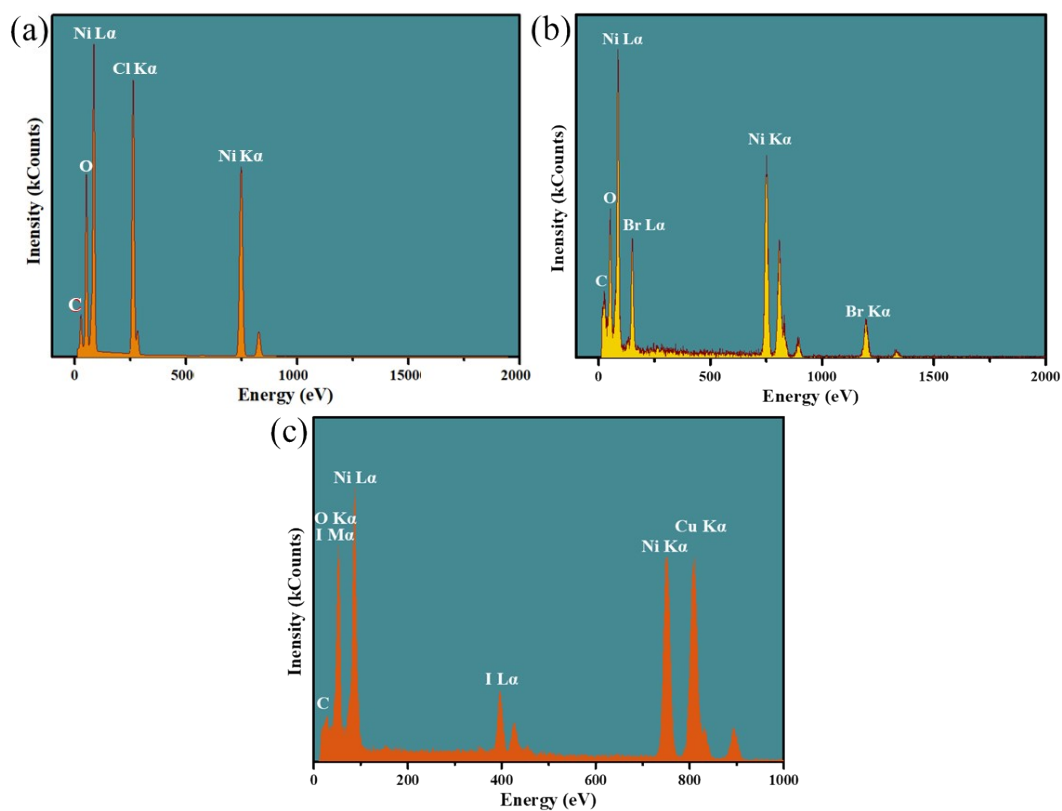


**Figure S2.** EDS spectra of (a) Ni(OH)Cl, (b) Ni(OH)Br, and (c) Ni(OH)I.

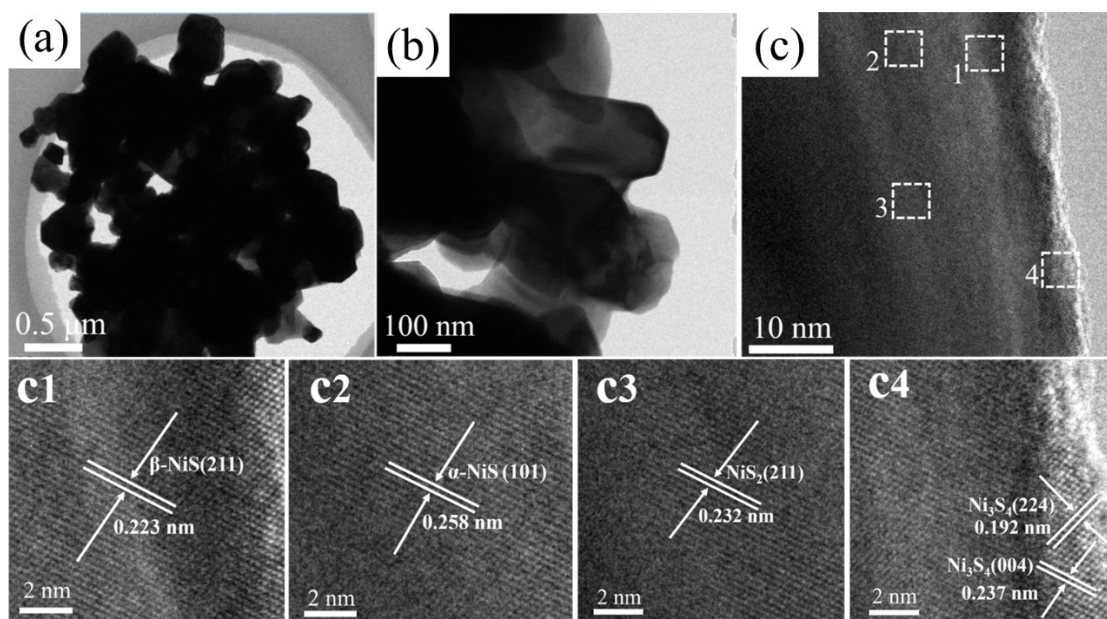


**Figure S3.** TEM images of S1.

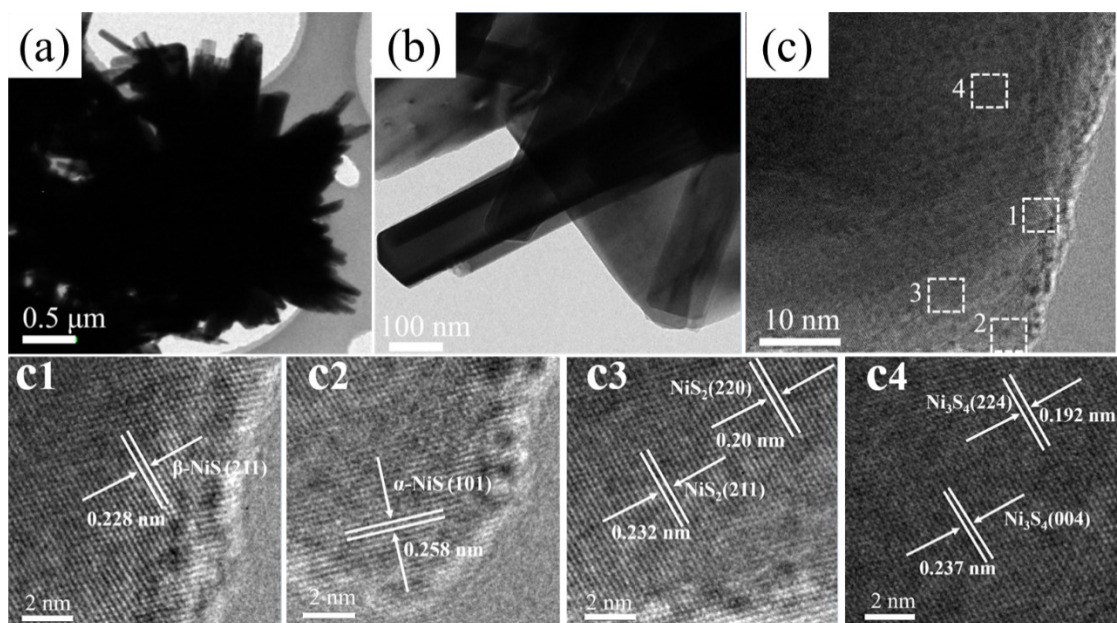


**Figure S4.** TEM images of S2.

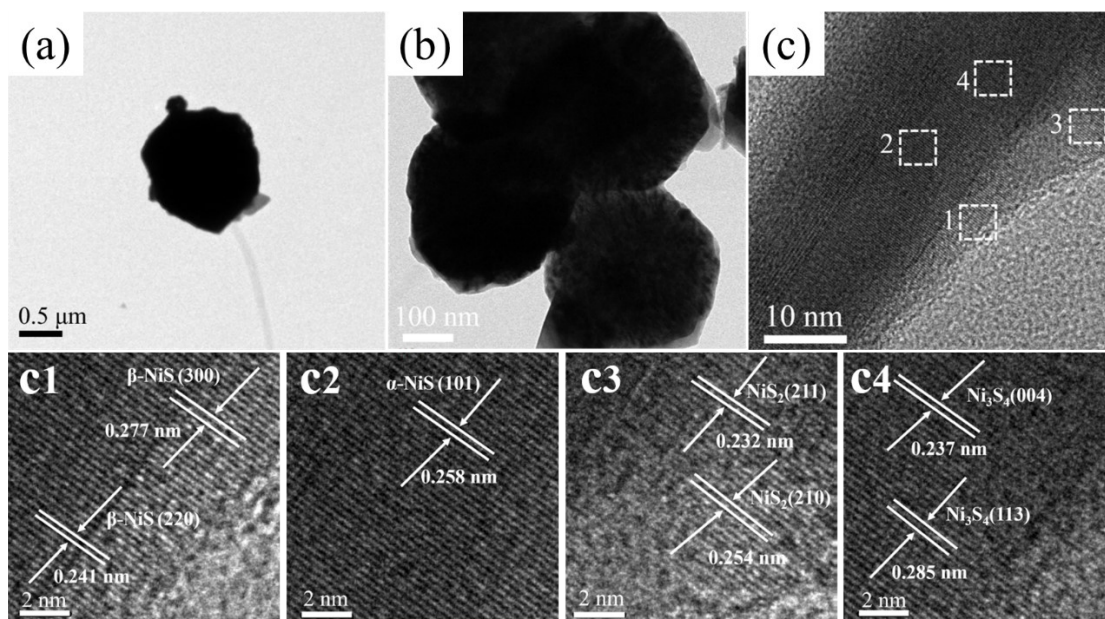


Figure S5. TEM images of S3.

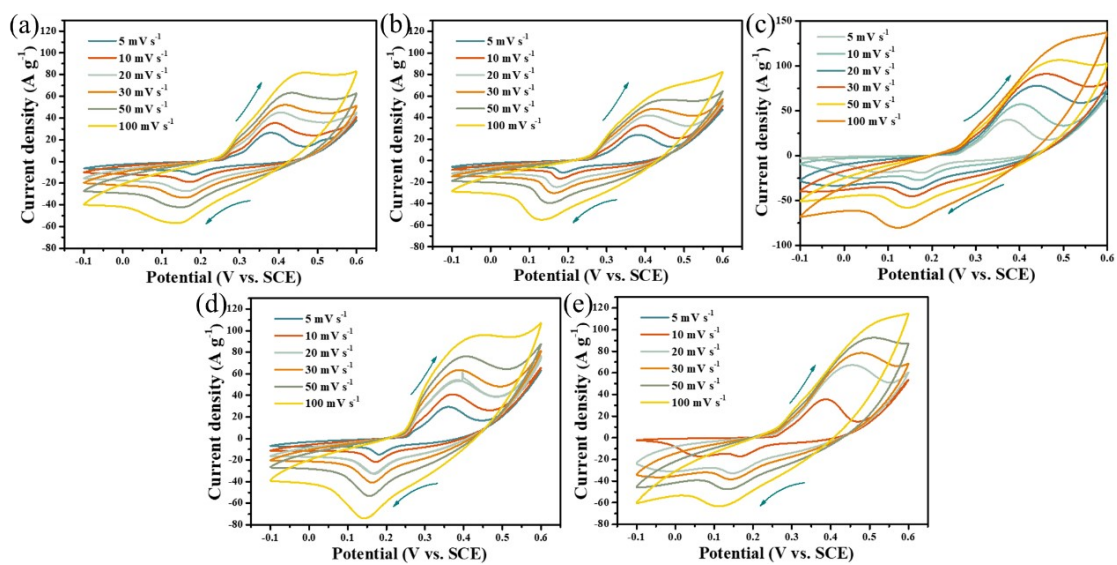


Figure S6. (a-e) CV curves of NS-1h, NS-3h, NS-6h, NS-12h, and NS-20h at different scan rates, successively.

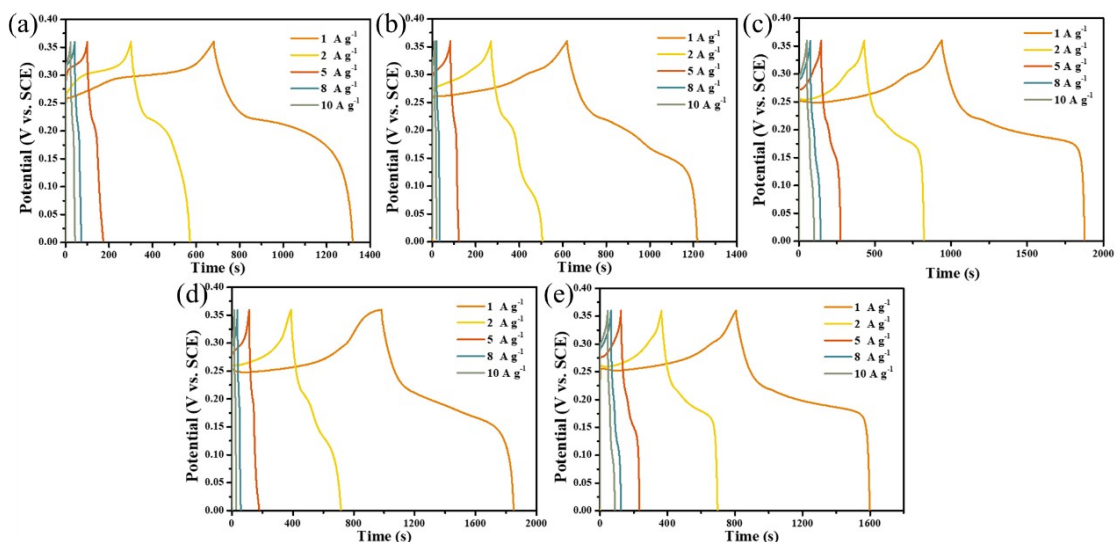


Figure S7. (a-e) GCD curves of NS-1h, NS-3h, NS-6h, NS-12h, and NS-20h at different scan rates.

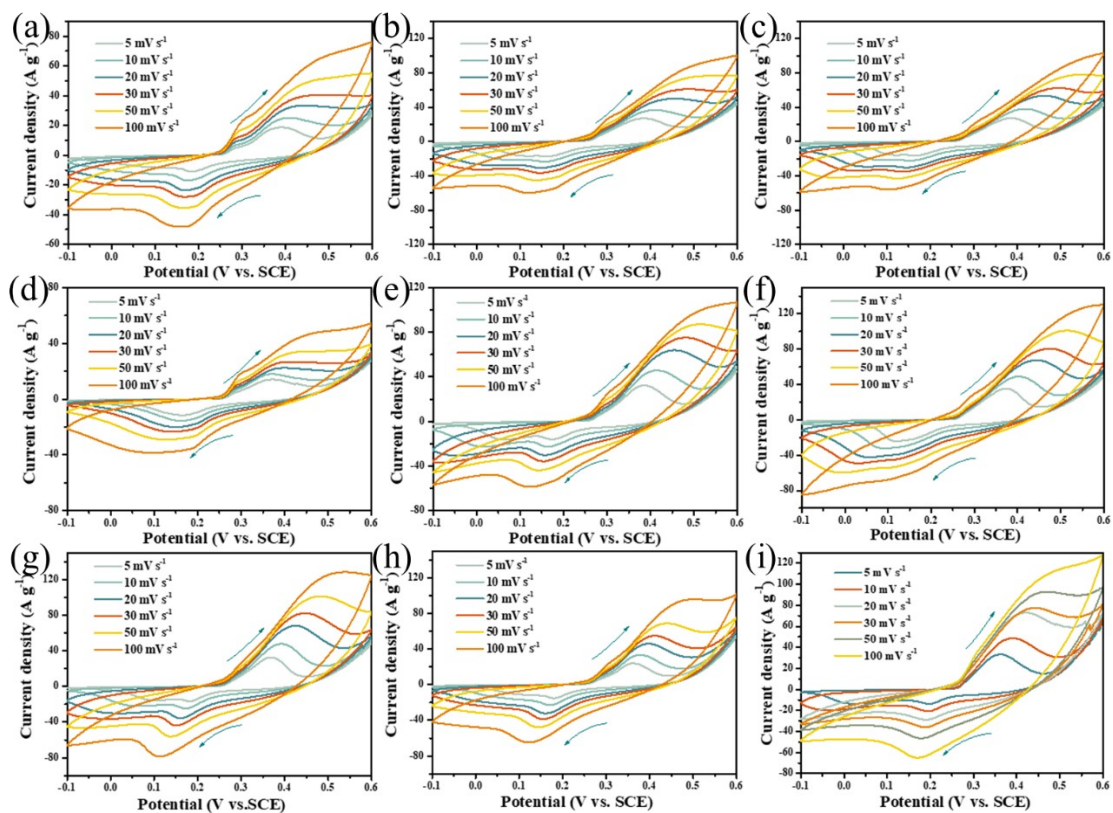


Figure S8. CV curves of N-1 to N-9.

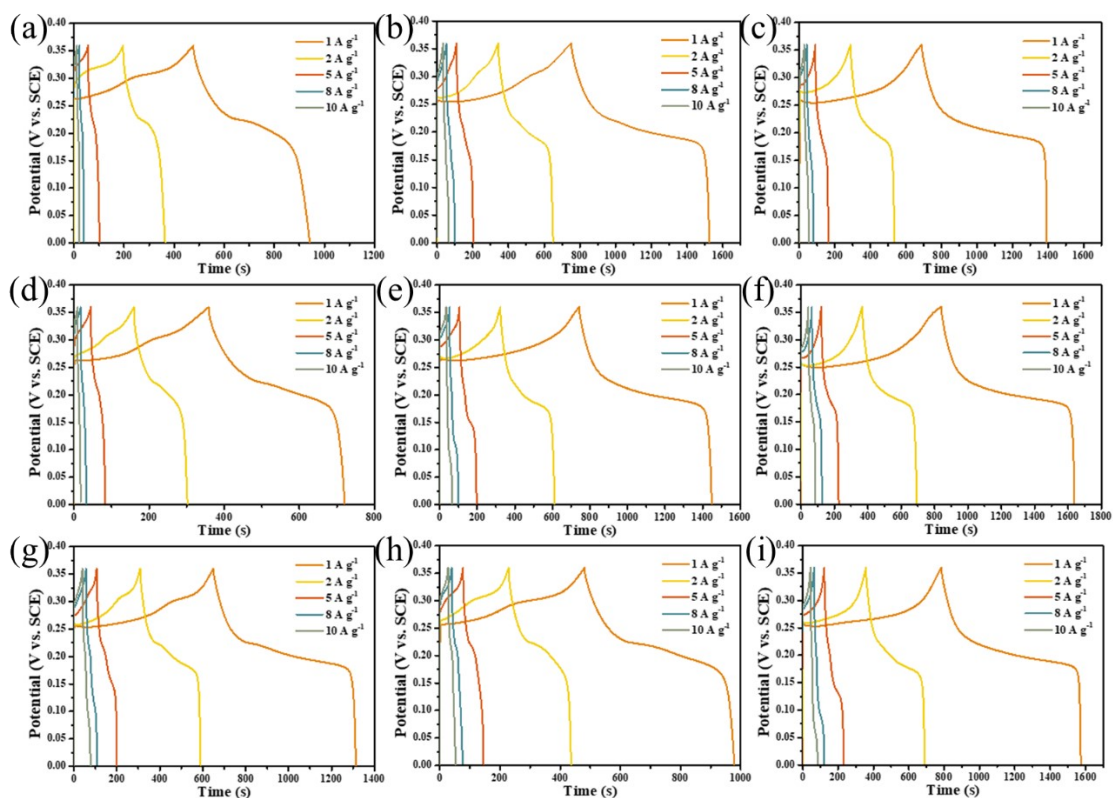


Figure S9. GCD curves of N-1 to N-9.

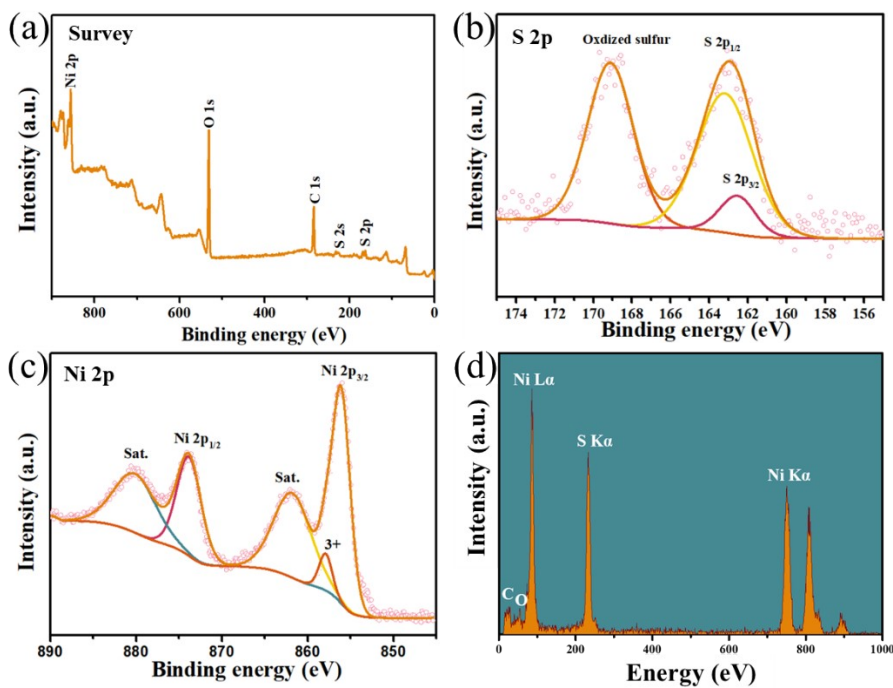
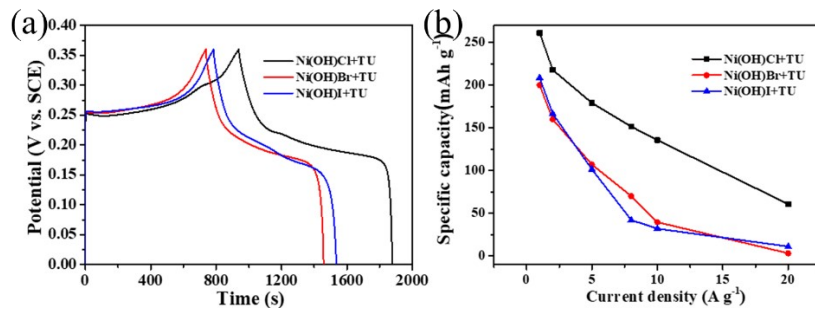
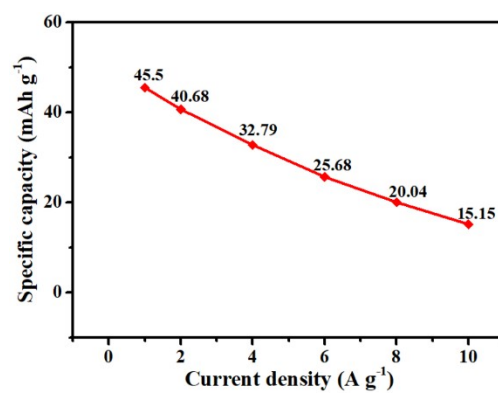


Figure S10. (a) Survey XPS spectrum of NCS. (b) S2p XPS spectrum of NCS. (c) Ni2p XPS spectrum of NCS. (d) EDS spectrum of NCS.



**Figure S11.** (a) GCD curves of NCS, NBS, and NIS. (b) Specific capacities of NCS, NBS, and NIS at diverse current densities.



**Figure S12.** Specific capacities of the fabricated supercapacitor at different current densities.

**Table S1.** L9(3<sup>4</sup>) orthogonal experimental data.

No.	Col. t (h)	A T (°C)	B -	C n(Ni(OH)Cl)/n(TU)	D C <sub>m</sub> mAh·g <sup>-1</sup>
1	1(6)	1(120)	1	1(0.15)	129.5
2	1	2(160)	2	2(0.3)	214
3	1	3(200)	3	3(1)	196.3
4	2(12)	1	2	3	100.7
5	2	2	3	1	196.1
6	2	3	1	2	222.4
7	3(20)	1	3	2	184.5
8	3	2	1	3	138.3
9	3	3	2	1	220.7
K <sub>1j</sub>	539.8	414.7	-	546.3	-
K <sub>2j</sub>	519.2	548.4	-	620.9	-
K <sub>3j</sub>	543.5	639.4	-	435.3	-
k <sub>1j</sub>	179.9	138.2	-	182.1	-
k <sub>2j</sub>	173.1	182.8	-	207.0	-
k <sub>3j</sub>	181.2	213.1	-	145.1	-
R	8.1	74.9	-	61.9	-
Factor Order	T > n(Ni(OH)Cl)/n(TU) > t				
Optimal Scheme	B <sub>3</sub> C <sub>2</sub> A <sub>3</sub>				

**Table S2.** Quantitative analysis of S1, S2, and S3 by XRD data.

Sample	Phase	Weight Percentage (%)
S1	$\beta$ -NiS	66.1
	$\text{Ni}_3\text{S}_4$	23.5
	$\alpha$ -NiS	8.2
	$\text{NiS}_2$	2.2
S2	$\beta$ -NiS	75.6
	$\text{Ni}_3\text{S}_4$	15.6
	$\alpha$ -NiS	5.7
	$\text{NiS}_2$	3.1
S3	$\beta$ -NiS	67.7
	$\text{Ni}_3\text{S}_4$	16.6
	$\alpha$ -NiS	7.4
	$\text{NiS}_2$	8.3

**Table S3.** A comparison of the specific capacity of nickel-based materials reported previously.

Sample	Capacity (mAh·g <sup>-1</sup> )	Current density (A·g <sup>-1</sup> )	Electrolyte	Ref.
5-NiS@CoS	168.1	1	2 M KOH	1
NiS-C	168.3	0.5	3 M KOH	2
NiCo <sub>2</sub> S <sub>4</sub> /Co <sub>9</sub> S <sub>8</sub> hollow nanospheres	126.0	1	1 M KOH	3
NiS nanostructures	120.5	1	2 M KOH	4
NiS hierarchical hollow cubes	133.6	1	2 M KOH	5
RHAC/NiCo <sub>2</sub> S <sub>4</sub>	233.3	1	2 M KOH	6
Ni <sub>3</sub> S <sub>4</sub> @rGO	203.3	2	2 M KOH	7
NiS/NiO	118.1	2	2 M KOH	8
NiS/NTA-2	191.3	1	2 M KOH	9
NiS@C QDs-CNTs-rGO	241.0	1	1 M KOH	10
Ni <sub>3</sub> S <sub>4</sub> -NiS/rGO	219.2	1	2 M KOH	11
H-NiS <sub>1-x</sub> /C-50	216.0	1	6 M KOH	12
R-NiS/rGO	206.6	1	2 M KOH	13
C@MoS <sub>2</sub> /Ni <sub>3</sub> S <sub>4</sub>	132.1	2	2 M KOH	14
Ni <sub>1-x</sub> Co <sub>2-x</sub> S/Co(OH) <sub>2</sub>	195.1	1	3 M KOH	15
Cu-doped Ni <sub>3</sub> S <sub>2</sub>	105.9	1	3 M KOH	16
Ni <sub>3</sub> S <sub>4</sub> -MoS <sub>2</sub>	136.8	1	3 M KOH	17
pyrite NiS <sub>2</sub> nanoparticles	163.9	2	6 M KOH	18
β-NiS@Ni	191.1	2	1 M KOH	19
NCS	261.2	1	2 M KOH	This work

**Table S4.** A comparison of some supercapacitors reported previously.

ECs	Energy density (Wh·kg <sup>-1</sup> )	Power density (W·kg <sup>-1</sup> )	Ref.
5-NiS@CoS//AC	24.1	752.15	1
NiS-C//AC	35.07	420.0	2
NiCo <sub>2</sub> S <sub>4</sub> /Co <sub>9</sub> S <sub>8</sub> hollow nanospheres//AC	36.7	800.0	3
NiS nanostructures//AC	16.5	250.0	4
NiS hierarchical hollow cubes//AC	34.9	387.5	5
RHAC/NiCo <sub>2</sub> S <sub>4</sub> /RHAC	41.6	150.0	6
Ni <sub>3</sub> S <sub>4</sub> @rGO//AC	37.3	398	7
NiS/NTA-2//AC	30.8	4187.2	9
NiS@C QDs-CNTs- rGO//Graphene	21.0	811	10
H-NiS <sub>1-x</sub> /C-50//AC	36.88	750	12
Ni <sub>1</sub> -Co <sub>2</sub> -S/Co(OH) <sub>2</sub> //AC	48.8	800	15
Cu-doped Ni <sub>3</sub> S <sub>2</sub> //AC	33.7	850.1	16
Ni <sub>3</sub> S <sub>4</sub> -MoS <sub>2</sub> //AC	58.43	385.95	17
pyrite NiS <sub>2</sub> nanoparticles//AC	54.2	940.0	18
β-NiS@Ni//AC	40.0	720.0	19
NCS//rGO	36.4	800.0	This work

## References

1. Miao, Y.; Zhang, X.; Zhan, J.; Sui, Y.; Qi, J.; Wei, F.; Meng, Q.; He, Y.; Ren, Y.; Zhan, Z.; Sun, Z., Hierarchical NiS@CoS with controllable core-shell structure by two-step strategy for supercapacitor electrodes. *Advanced Materials Interfaces* **2020**, *7* (3), 1901618.
2. Harish, S.; Naveen, A. N.; Abinaya, R.; Archana, J.; Ramesh, R.; Navaneethan, M.; Shimomura, M.; Hayakawa, Y., Enhanced performance on capacity retention of hierarchical NiS hexagonal nanoplate for highly stable asymmetric supercapacitor. *Electrochimica Acta* **2018**, *283*, 1053-1062.
3. Shen, Y.; Zhang, K.; Chen, B.; Yang, F.; Xu, K.; Lu, X., Enhancing the electrochemical performance of nickel cobalt sulfides hollow nanospheres by structural modulation for asymmetric supercapacitors. *Journal of Colloid and Interface Science* **2019**, *557*, 135-143.
4. Nandhini, S.; Muralidharan, G., Facile microwave-hydrothermal synthesis of NiS nanostructures for supercapacitor applications. *Applied Surface Science* **2018**, *449*, 485-491.
5. Ma, X.; Zhang, L.; Xu, G.; Zhang, C.; Song, H.; He, Y.; Zhang, C.; Jia, D., Facile synthesis of NiS hierarchical hollow cubes via Ni formate frameworks for high performance supercapacitors. *Chemical Engineering Journal* **2017**, *320*, 22-28.
6. Wang, H.; Wu, D.; Zhou, J., Gasified rice husk based RHAC/NiCo<sub>2</sub>S<sub>4</sub> composite for high performance asymmetric supercapacitor. *Journal of Alloys and Compounds* **2019**, *811*, 152073.
7. Hu, Q.; Zou, X.; Huang, Y.; Wei, Y.; YaWang; Chen, F.; Xiang, B.; Wu, Q.; Li, W., Graphene oxide-drove transformation of NiS/Ni<sub>3</sub>S<sub>4</sub> microbars towards Ni<sub>3</sub>S<sub>4</sub> polyhedrons for supercapacitor. *Journal of Colloid and Interface Science* **2020**, *559*, 115-123.
8. Wang, Y.; Pan, A.; Zhang, Y.; Shi, J.; Lin, J.; Liang, S.; Cao, G., Heterogeneous NiS/NiO multi-shelled hollow microspheres with enhanced electrochemical performances for hybrid-type asymmetric supercapacitors. *Journal of Materials*

*Chemistry A* **2018**, *6* (19), 9153-9160.

9. Wu, D.; Xie, X.; Ma, Y.; Zhang, J.; Hou, C.; Sun, X.; Yang, X.; Zhang, Y.; Kimura, H.; Du, W., Morphology controlled hierarchical NiS/carbon hexahedrons derived from nitrilotriacetic acid-assembly strategy for high-performance hybrid supercapacitors.

*Chemical Engineering Journal* **2021**, 133673.

10. Zhang, R.; Lu, C.; Shi, Z.; Liu, T.; Zhai, T.; Zhou, W., Hexagonal phase NiS octahedrons co-modified by 0D-, 1D-, and 2D carbon materials for high-performance supercapacitor. *Electrochimica Acta* **2019**, *311*, 83-91.

11. Azizi Darsara, S.; Seifi, M.; Askari, M. B.; Osquian, M., Hierarchical 3D starfish-like Ni<sub>3</sub>S<sub>4</sub>-NiS on reduced graphene oxide for high-performance supercapacitors. *Ceramics International* **2021**, *47* (15), 20992-20998.

12. Huang, C.; Gao, A.; Yi, F.; Wang, Y.; Shu, D.; Liang, Y.; Zhu, Z.; Ling, J.; Hao, J., Metal organic framework derived hollow NiS@C with S-vacancies to boost high-performance supercapacitors. *Chemical Engineering Journal* **2021**, *419*, 129643.

13. Qu, C.; Zhang, L.; Meng, W.; Liang, Z.; Zhu, B.; Dang, D.; Dai, S.; Zhao, B.; Tabassum, H.; Gao, S.; Zhang, H.; Guo, W.; Zhao, R.; Huang, X.; Liu, M.; Zou, R., MOF-derived  $\alpha$ -NiS nanorods on graphene as an electrode for high-energy-density supercapacitors. *Journal of Materials Chemistry A* **2018**, *6* (9), 4003-4012.

14. Qin, S.; Yao, T.; Guo, X.; Chen, Q.; Liu, D.; Liu, Q.; Li, Y.; Li, J.; He, D., MoS<sub>2</sub>/Ni<sub>3</sub>S<sub>4</sub> composite nanosheets on interconnected carbon shells as an excellent supercapacitor electrode architecture for long term cycling at high current densities. *Applied Surface Science* **2018**, *440*, 741-747.

15. Xu, T.; Li, G.; Zhao, L., Ni-Co-S/Co(OH)<sub>2</sub> nanocomposite for high energy density all-solid-state asymmetric supercapacitors. *Chemical Engineering Journal* **2018**, *336*, 602-611.

16. Li, G.; Cui, X.; Song, B.; Ouyang, H.; Wang, K.; Sun, Y.; Wang, Y., One-pot synthesis of Cu-doped Ni<sub>3</sub>S<sub>2</sub> nano-sheet/rod nanoarray for high performance supercapacitors. *Chemical Engineering Journal* **2020**, *388*, 124319.

17. Luo, W.; Zhang, G.; Cui, Y.; Sun, Y.; Qin, Q.; Zhang, J.; Zheng, W., One-step extended strategy for the ionic liquid-assisted synthesis of Ni<sub>3</sub>S<sub>4</sub>-MoS<sub>2</sub> heterojunction

electrodes for supercapacitors. *Journal of Materials Chemistry A* **2017**, *5* (22), 11278-11285.

18. Zhang, J.; Zhang, D.; Yang, B.; Shi, H.; Wang, K.; Han, L.; Wang, S.; Wang, Y., Targeted synthesis of NiS and NiS<sub>2</sub> nanoparticles for high-performance hybrid supercapacitor via a facile green solid-phase synthesis route. *Journal of Energy Storage* **2020**, *32*, 101852.

19. Bhagwan, J.; Khaja Hussain, S.; Krishna, B. N. V.; Yu, J. S.,  $\beta$ -NiS 3D micro-flower-based electrode for aqueous asymmetric supercapacitors. *Sustainable Energy & Fuels* **2020**, *4* (11), 5550-5559.